Research on melanoma image segmentation by incorporating medical prior knowledge

Hong Zhao [1], **Aolong Wang** [Corresp., 1], **Chenpeng Zhang** [1]

[1] School of Computer and Communication, Lanzhou University of Technology, Lanzhou, Gansu, China

Corresponding Author: Aolong Wang
Email address: wang_aolong_0403@163.com

Background: Melanoma image segmentation has important clinical value in the diagnosis and treatment of skin diseases. However, due to the difficulty of obtaining data sets, and the sample imbalance, the quality of melanoma image data sets is low, which reduces the accuracy and the effectiveness of computer aided diagnosis of melanoma image.

Objective: In this work, a method of melanoma image segmentation by incorporating medical prior knowledge is proposed to improve the fidelity of melanoma image segmentation.

Methods: Anatomical analysis of the melanoma image reveal the star shape of the melanoma image, which can be encoded into the loss function of the UNet model as a prior knowledge.

Results: Our experimental results on the ISIC-2017 data set demonstrate that the model by incorporating medical prior knowledge obtain a mIoU (Mean Intersection over Union) of 87.41%,a Dice Similarity Coefficient of 93.49%.

Conclusion: Therefore, the model by incorporating medical prior knowledge achieve the first rank in the segmentation task comparing to other models and has high clinical value.

Research on Melanoma Image Segmentation by Incorporating Medical Prior Knowledge

Hong Zhao[1], Aolong Wang[1], Chenpeng Zhang[1]

[1] School of Computer and Communication, Lanzhou University of Technology, Lanzhou, Gansu, China

Corresponding Author: Aolong Wang
Email Address:wang_aolong_0403@163. com

Abstract

Background: Melanoma image segmentation is of great important clinical value in the diagnosis and treatment of skin diseases. However,due to the difficulty of obtaining melanoma image data sets,and the unbalanced sample and poor data quality,the accuracy of melanoma image segmentation is low, which affects the disease diagnosis.

Objective: In this work,a method of melanoma image segmentation by incorporating medical prior knowledge is proposed to improve the fidelity of melanoma image segmentation.

Methods: Anatomical analysis of the melanoma image reveals that the melanoma images where lesions occur have a star shape,which can be encoded into the loss function of the UNet model as a prior knowledge.

Results: Our experimental results of the model on the ISIC-2017 melanoma dataset demonstrate that the model by incorporating medical prior knowledge can obtain mIoU(Mean Intersection over Union) of 87. 41% and a Dice Similarity Coefficient of 93. 49%.

Conclusion: Therefore,the model by incorporating medical prior knowledge achieve the first rank in the segmentation task compared to other models and has high clinical value.

Introduction

Melanoma is the most common type of skin cancer and has the highest death rate of all skin cancers. However, melanoma can be cured with a minor surgical operation detected at an early stage. Therefore,segmentation of melanoma images can be used to help dermatologists evaluate and take treatment means as soon as possible.

Initially, basic methods with low segmentation accuracy such as edge detection, threshold segmentation and region segmentation were introduced to segmentation of medical images. With the rapid development of deep learning technology, deep learning models have been widely leveraged in segmentation of skin lesions. However,with the improvement of model accuracy, complex structures and models are increasingly dependent on the number of images and high-

- -

40   quality of them, which is extremely difficult to get. The most common techniques to increase the
41   number of images are data augmentation, such as traditional visual augmentation methods or
42   generative models.
43   In the context of applying models on low-quality data sets[1-6],the most common
44   techniques are data augmentation,such as traditional visual augmentation methods or generative
45   models [7]. However,these methods only use the data set itself and do not introduce external
46   information into models. Despite the success of augmentation based techniques,the problems of
47   low-accuracy persist. To solve this problem, medical prior knowledge can be introduced into the
48   segmentation model [8] to improve the performance of the segmentation map,such as transfer
49   learning, using multi-modal data sets,and incorporating physicians' knowledge. The most
50   effective method is to combine physicians' knowledge,that is,using physicians' medical domain
51   knowledge of doctors for model training before segmentation,during or after segmentation. For
52   example,imitating the training patterns of physicians and prioritizing the diagnosis of more
53   severe samples during training[9]. Or use the general diagnostic mode of doctors[10].
54   Since real physicians often do not need a large amount of data to make diagnoses, this
55   method can bypass the problem of reliance on high-quality medical image data sets.
56   However,while the above methods are applied to the segmentation of melanoma
57   images,segmentation results that are obviously inconsistent with the anatomical structure of skin
58   lesions,Internal hole errors and external island errors occur in the segmentation map. The use of
59   loss functions that do not encode anatomical priors led to these errors.
60   To solve this problem,specific shape constraints can be designed according to the speckle
61   shape of the melanoma images and utilized to the model can be trained using that. Since the
62   seminal work of O. Veksler,the star shape prior has been leveraged in the graph cut algorithm.
63   Literature[11] is one of the pioneering work to incorporating star shape priors into segmentation
64   of skin lesion images. They encoded the star shape prior into the loss function to improve the
65   convexity of the segmentation map. However,this method is not powerful enough to penalize the
66   internal error pixels in the prediction map,which will lead to the internal hole errors in the
67   segmentation map. The acuracy of the model is reduced by using this approach.
68   We aim to proposes a melanoma image segmentation method based on star shape
69   prior,and encode it in loss function as a regularization term. To penalize non-star shape
70   segment,including external and internal errors area. our experimental results demonstrate the
71   improvement of segmentation performance.
72

73 **Materials & Methods**
74 **1. Encoding regularization term in the loss function as prior knowledge.**
75 **1. 1 Encoding prior regularization term in the loss function**
76   Comparing with the segmentation of ordinary images,there is a lot of many anatomical
77   prior informations in medical images such as the position,shape and topological structure of
78   organs or lesions. There are several methods and techniques to incorporating anatomical priors of
79   lesions or organs into the model of medical image segmentation. It is one of the methods by

80   learning prior knowledge with generative model and then integrating it into the network[16].
81   Alternatively,the fuzzy results of segmentation map[17] can be refined. However,these methods
82   need to be carried out in the pre-processing or post-processing stage and cannot be trained end-
83   to-end.
84   An end-to-end training model is to encoding anatomic prior knowledge to the loss
85   function as a regularization term. The prior features can be divided into the following categories
86   according to the types of regularization term:topological regularization term,which ignore the
87   shape of organs and extract abstract connections between organs;dimensional regularization
88   terms,which combine dimensional information about the size of organs or lesions in the
89   model;interregional regularization terms are to find the geometrical and distance interaction
90   between image regions;Shape regularization term,such as geometric shape feature,polygon
91   feature,star feature,etc.
92   Different regularization terms should be designed for different organ and lesion when
93   encoding medical prior into the loss function. Topological priors should be used when encoding
94   the features of thin films and curved objects. For the tasks of whole-body
95   segmentation,interregional priors are needed;For skin lesions,such as melanoma
96   segmentation,star priors can be used to improve the convexity of organs or lesions to enhancing
97   the model performance.
98   In Figure 1,Figure 1(a),(c),(e) and (g) demonstrate the original image of melanoma
99   segmentation,and Figure 1(b),(d),(f) and (h) are the corresponding segmentation labels. As
100   shown in Figure 1, the color distribution of melanoma lesion sites on the image is asymmetric,
101   leading to degraded segmentation results of the previous model. However,due to malignant
102   melanoma lesion has the anatomical speckled shape,dermatologists often mark the locations of
103   lesions in melanoma images with a star shape. Therefore,it is suitable to encoding star-shaped
104   regularization term to avoid the inner hole error and the outer island error commonly seen in
105   melanoma segmentation models.

106   **1. 2 Star convex set**

107   Melanoma skin lesions have a speckled shape. The Star-shaped prior is suitable for the
108   segmentation of skin lesions. Star-shaped prior is derived from the concept of star convex set in
109   mathematics,as shown in Figure 2. For a sample of malignant melanoma image,all pixels on the
110   image form pixel space Ω. If all the focal pixels on it form a set y,the center of the set is the
111   point c. Then,the conditions for identifying y as a star convex set is that:At any point p of the
112   set y,its line with c at any point q in l_{pc} is also in y.

113   **2. Melanoma image segmentation using star prior encoded loss function**

114   There are usually only a few dozens to a few hundreds of malignant melanoma images in
115   a melanoma image data set,which is too small. If only the data set itself is used for image
116   segmentation,the segmentation results will not be able confirm the anatomical characteristics of
117   melanoma skin lesions. Therefore,the UNet model is first constructed in this paper. And then
118   segmented star prior loss function was designed for training to enhance the performance of the
119   model.

2. 1 Loss function without prior knowledge

There are different type of loss functions without coding anatomic priors,such as cross-entropy loss,Dice loss and Kappa loss,etc. The cross-entropy loss function is the most commonly used loss function in segmentation of skin lesions. However,it ignores the quantity ratio of different types of pixels in the sample space. Therefore, it is easy to produce the problem of category imbalance,and the category with the most pixels leads the training inevitably. The Dice loss function can be used to balance positive and negative samples. It has good performance when positive and negative samples are extremely uneven,and the loss of each pixel is strongly correlated with the adjacent region. However,the Dice loss function has the problem of insufficient mining of background area. It will adversely affect the back propagation process,making training process unstable. Therefore,Zhang J. et al. proposed the Kappa loss function[12],whose calculation method included all pixels in the image map,even a large number of true negative pixels not involved in other loss functions. The Kappa loss function further improved the segmentation accuracy and model convergence. In addition,new Loss functions such as Focal Loss function[13] and Conservative Loss(CL) function[14] were proposed.

Although these attempts and improvements on loss function have enhanced the segmentation model performance recently,there are still shortcomings as follows[15]:First, these methods ignore the advanced characteristics of lesion location and medical structure. Such as shape and topological structure;Second,they equally penalize all kinds of error pixels in the image segmentation map. While utilizing the above loss functions and using the common segmentation models in segmentation,this model can not take advantage of a particular organ or pathological changes of anatomy structure and the spatial relationship between organs. Therefore, in the segmentation of melanoma images,results that are obviously inconsistent with the anatomical structure of skin lesions. Errors Including internal hole and external island often appear. In Figure 3,Figures 3(a) and (b) show the internal hole error,and Figures 3(c) and (d) show the external island error. Although hybrid loss functions have been used recently to obtain high performance [23], we prefered incorporation of prior knowledge to improve efficiency and robustness.

2. 2 UNet structure

The malignant sample data in the original data set is selected for training. The UNet model is built with ResNet34 as the backbone for image segmentation of malignant samples. Its structure is shown in Figure 4.

In Figure 4,the UNet model is divided into an upward path and downward path according to the depth of convolutional layers. The upward path is used to obtain context information,and the downward path is used to locate targets. The high level informations of the network has low resolution but rich semantic information. While The high resolution of low-level informations provide more detailed edge information for segmentation map. Due to such characteristics,the UNet model is suitable for medical image segmentation. Its skip connections structure can not only get high-level semantic informations,but also extract the underlying informations of convolutional network,which conforms to the characteristics of simple semantic information of

160   medical image. The malignant sample data are divided into training set,evaluation set and test set
161   according to a certain proportion. The UNet model based on ResNet34 backbone is built to
162   obtain the location of lesions in the malignant melanoma sample images.

163   **2. 3 Star prior loss function applied to segmentation of melanoma**

164   In order to encode the anatomical structure of melanoma skin lesions into the UNet
165   model for training. Shape prior can be fused into the loss function. When the star prior is
166   encoded into the loss function,it can be designed by numerical superposition,as shown in
167   Formula (1)[11].

$$\theta^* = \arg\min_{\theta} L(X,Y;\theta)$$

168   (1)

$$L(X,Y;\theta) = \alpha L_{ce} + \beta L_{sh}$$

169   In Formula (1), θ represents the UNet parameters, X and Y represents the predicted
170   segmentation map and the segmentation label map respectively. While parameter θ is
171   continuously optimized until it converges to the final value θ^*. In reference [9], L_{ce} represents
172   the cross-entropy loss function. It is composed of two parts, L_{ce} and L_{sh} ,multiplied by weights α
173   and β respectively and added together.You can set α to 1 and then adjust the value of β. A and
174   B are set in the way of hyperparameters before training,where L_{ce} can be replaced by other loss
175   functions commonly used in medical image segmentation,such as Dice loss function.

176   According to the features of the internal hole errors and external island errors in
177   melanoma image segmentation,the star prior formula regularization term L_{sh} is designed,as
178   shown in Formula (2).

$$L_{sh}(X,Y;\theta) = \begin{cases} \dfrac{1}{Nn_\Omega}\sum_{i=1}^{N}\sum_{p\in\Omega}\sum_{q\in l_{pc}} \mu*A*B*\dfrac{1}{l_{qc}}, & \text{y}_{ip}=1 \text{ and } P(\text{y}_{ip}=1|x(i);\theta)<0.5 \text{ and PsN(q)<0} \\[2ex] \dfrac{1}{Nn_\Omega}\sum_{i=1}^{N}\sum_{p\in\Omega}\sum_{q\in l_{pc}} \rho*A*B*\dfrac{1}{l_{qc}}, & \text{y}_{ip}=1 \text{ and } P(\text{y}_{ip}=1|x(i);\theta)<0.5 \text{ and PsN(q)>=0} \\[2ex] \dfrac{1}{Nn_\Omega}\sum_{i=1}^{N}\sum_{p\in\Omega}\sum_{q\in l_{pc}} A*B*C, & \text{otherwise} \end{cases}$$

179   (2)

$$A = \begin{cases} 1, & \text{if } \text{y}_{ip} = \text{y}_{iq} \\ 0, & \text{otherwise} \end{cases}$$

$$B = \left| \text{y}_{ip} - P(\text{y}_{ip}-1|x(i);\theta) \right|$$

$$C = \left| P(\text{y}_{ip}=1|x(i);\theta) - P(\text{y}_{iq}=1|x(i);\theta) \right|$$

180   Where N is the total number of samples, Ω is the pixel space of a melanoma image
181   sample, n_Ω is the total number of pixel points in the pixel space Ω. The location of the focus
182   point is c ,while p is any point of pixel space Ω ,and q is a point on line l_{pc}. y_{ip} and y_{iq}
183   represent the label of the points p and q ,while y_{ip} and y_{iq} represent the model predicted
184   values of points p and q respectively. This symbol * represents matrix multiplication.

185    $PsN()$ function is used to discriminate whether a point q is an internal hole point. To be
186   specific,it is to connect point c and point q first,and then take the outward ray starting from
187   point q until they touch the edge of the image map. As shown in Figure 5,Figure 5 (a) is the
188   segmentation label map of the melanoma image,and the blue part in Figure 5 (b) represents the
189   prediction map of lesion location by model,where the positions marked in yellow are the
190   segmentation error. The focus of line l_{qn} and internal hole error is r. If the length of line l_{rn} is
191   greater than that the length of line l_{rq},point q is identified as the internal hole error point,namely
192    $PsN(q)>=0$;otherwise,point q is identified as the edge false negative error point,namely
193    $PsN(q)<0$.
194   In the medical image segmentation tasks,the errors are divided into two kinds,namely the
195   false positive errors and false negatives errors. Then further subdivided into four categories:the
196   internal false negative,the edge false negative,the external false positive and the edge false
197   positive,as shown in Figure 6. $p1$, $p2$, $p3$ and $p4$ are classified as edge false negative
198   error,edge false positive error,internal hole error and the external island errors. In melanoma
199   image segmentation,internal false negative (internal hole) errors and external false positive
200   (external island) errors should be penalized. Therefore,L_{sh} was designed as a piecewise
201   function,divided into three parts. In formula (2),the first formula is designed to regularize the
202   edge false negative errors,the second formula is applied to regularize the internal hole errors,and
203   the third formula is used to normalize the other outer errors. The hyperparameters μ and ρ are
204   set separately before training and regularization with different intensities was applied to different
205   kinds of errors.
206   The optimization goal of the star prior loss function L_{sh} is to assign the same label to all q
207   points on the line l_{cp} as to point p,on the condition that the labels of point p and point q must
208   be the same. Therefore,item A is designed to be 1 only when the true value of point p and point
209   q are the same. Otherwise,the value will be 0,which means that no shape regular term is
210   encoded. Item B represents the difference between the real value and the predicted values at
211   point p ,so item B sets the strength of the regularization term for L_{sh}. The more severe the
212   prediction error at point p is compared to the real situation,the larger the regularization term
213   is,and the heavier the penalty for the error is. A and B are divided by l_{qc} when calculating the
214   regularization item. Because the point q and the distance between the center point c will affect
215   the value of the regularization item. If the internal hole error exists segmentation image near the
216   center,the accumulative losses at each point q makes the regularization item too small. Then the
217   loss function cannot achieve the purpose of penalizing these errors;Secondly, the false negative
218   error points near the edge of the real segmentation label are too far away from the center point c
219   ,resulting in excessive regularization after loss accumulation. In terms A and B ,the center

220   distance is scaled by dividing by l_{qc} to remove the influence caused by the distance between

221   point q and point c. Instead, μ and ρ are used to control the value of the regularization

222   term,so as to improve the accuracy.

223   C sets the way of regularizing the loss function in melanoma lesions. Using the functions

224   as shown in formula (1) and formula (2),which can focus on the penalization of similar error

225   points in Figure 6 and $p3$ and $p4$. It regularize the final shape of the segmentation map into a

226   star shape,in accordance with the anatomical structure of the melanoma images.

227

228   **Results**

229   **1. Experimental design**

230   **1. 1Data set.**   The Society for Medical Impact Informatics(SIIM) has collaborated with the

231   International Skin Imaging Collaboration(ISIC),has constructed the largest open library of

232   images of skin lesions. The ISIC Melanoma Data set[16] is referred to as ISICM. The ISICM

233   contains 10,000 dermatoscopic images of skin lesions totally. Each of which is accompanied by a

234   professionally described and segmented image. ISICM is divided into benign and malignant

235   categories according to the disease description,and only 220 images of malignant melanoma

236   were concluded in this data set.

237   In our work,the model is applied to the preprocessed ISICM data set to build a three-stage

238   processing structure. And the ISICM was finely segmented. Finally,our experiment is

239   demonstrated in images,then the performance of the model is analyzed.   220 malignant sample

240   images were segmented in the proportion of 6:2:2 to the training set,the evaluation set and the

241   test set.

242   **1. 2Preprocessing.**   First,the images is scaled to a size of 256×X or Y×256 in accordance with

243   the length and width ratio of the image(X and Y are the height and weight of the scaled image.

244   scale final height and weight in the same proportion as the original image). The edges are then

245   filled and the image size is 256×256. In addition,the image is flipped and brightness adjusted.

246   Three malignant samples after data pretreatment are shown in Figure 7.

247   **1. 3Implementation details.**   The Pytorch framework [14] was used to implement this method.

248   Adam was selected as the optimizer during the training process. The initial learning rate was set

249   in 1E-3. In our experiment,400 epochs were trained. ImageNet pre-trained model[20] was used

250   for freezing training for the first 100 epochs,then learning rate attenuation was applied for the

251   last 200 epochs during training[21],in which every 5 epochs were attenuated to 95% of the

252   original learning rate. When the model is tested,the output of the model is taken as the final

253   result without any subsequent processing. Our model was run on a NVIDIA GTX1060.

254   **2. Ablation experiments**

255   For the core experiment, three groups of ablation experiments were designed, namely, the non-

256   regular term group, the unsegmented star prior group and the non-central distance scaling group.

257   The experimental results are shown in Table 1.

258   The segmentation results are displayed, as shown in Figure 8.

259 **2. 1Non regularization term group(baseline) .** As the baseline experimental group,the loss
260 function with star priori was not used,and only Dice loss function was used for training. As
261 shown in Figure 8 (c),due to the absence of shape regularization,the segmentation results do not
262 conform to the anatomical structure of melanoma,resulting in poor accuracy.

263 **2. 2Unsegmented star prior group.** Unsegmented basic star prior formula. Item L_{sh} design is
264 shown in Formula (3).

$$L_{sh}(X,Y;\theta) = \sum_{i=1}^{N} \sum_{p \in \Omega} \sum_{q \in l_{pc}} B^i{}_{pq} \times |y_{ip} - P(y_{ip} = 1 | X(i);\theta)|$$

265
$$\times |P(y_{ip} = 1 | X(i);\theta) - P(y_{iq} = 1 | X(i);\theta)|; \tag{3}$$

$$B^i{}_{pq} = \begin{cases} 1, & if\ y_{ip} = y_{iq} \\ 0, & otherwise \end{cases}$$

266   As shown in Figure 8 (d), the unsegmented star prior term uses the same regularization
267 term to penalize all errors that do not conform to the anatomical structure of the lesions,leading
268 to the difficulty in selecting weights α and β when designing the L_{sh} term,and to penalize the
269 segmentation errors of internal hole and external island with appropriate size. Because the loss
270 function does not use the segmentation function for various kinds of errors, the segmentation
271 result is reduced.
272 **2. 3non-Center distance scaling group.** The segmented star prior loss function in formula(1)
273 and formula(2) is applied for training,but l_{qc} is no division at the end of items A and item B .
274 Only the parameters μ and ρ are used to control the value of the regularization term. As shown
275 in Figure 8 (e),because each point q in the segmentation map and the distance between the
276 center point c each are not identical. That will have an effect on the value of the regularization
277 item,so using no L_{sh} center distance scaling way designs, μ and ρ , regardless of what
278 parameters the model select will cause a dramatic performance results decline. The performance
279 is even lower than the non regularization terms group.
280 **2. 4Segmented star prior group.** The segmented star prior loss function in Formula (1) and
281 Formula (2) was used for training,and the results were shown in Figure 8 (f). The segmentation
282 results were consistent with the anatomical results of melanoma with high accuracy. Using this
283 improved loss function, the convexity of the shape can be enhanced.
284 **3. Compare with other segmentation models**
285 Compared with UNet fused star prior method SSPFCN[6],Attention UNet[4] and dense
286 convolution method FC-densenet[22] on the ISICM data set,the results are shown in Table 2.
287 Previous methods performed well on large,high-quality data sets,but performed poorly on ISIC
288 data set with only 220 skin images of malignant melanoma. Comparing to the recent methods,the
289 star priority-based melanoma segmentation method has further improved the performance of the
290 segmentation model on the data set with fewer samples. An advantage of the proposed approach

291   is that a separate intensity normalization stage[24], which usually leads to increase the
292   computational complexity, is not needed.
293

Conclusions

295   In this work,a melanoma segmentation method incorporating medical prior is
296   proposed,and experimental verification is carried out on ISICM data set. Piecewise loss function
297   of star prior is designed and applied to melanoma image segmentation teak. Our experiment
298   demonstrate that the melanoma segmentation model based on the star prior enhances the
299   performance of the model,and improves the mIoU value,mAP value, Dice value and Jaccard
300   value.

301

302

303

References

305   [1]BADRINARAYANAN V, KENDALL A, CIPOLLA R. Segnet: A deep convolutional
306   encoder-decoder architecture for image segmentation[J]. IEEE Transactions on Pattern Analysis
307   and Machine Intelligence, 2017, 3{Ronneberger, 2015 #138}9(12): 2481-2495.
308   [2]RONNEBERGER O, FISCHER P, BROX T. U-net: Convolutional networks for biomedical
309   image segmentation[C]//International Conference on Medical Image Computing and Computer-
310   assisted Intervention. Springer, Cham, 2015, 9351: 234-241.
311   [3]ZHOU Z, SIDDIQUEE M M R, TAJBAKHSH N, et al. Unet++: A nested u-net architecture
312   for medical image segmentation[M]//Deep Learning in Medical Image Analysis and Multimodal
313   Learning for Clinical Decision Support. Springer, Cham, 2018, 11045: 3-11.
314   [4]OKTAY O, SCHLEMPER J, FOLGOC L L, et al. Attention u-net: Learning where to look
315   for the pancreas[J]. arXiv preprint arXiv:1804. 03999, 2018.
316   [5]ALOM M Z, HASAN M, YAKOPCIC C, et al. Recurrent residual convolutional neural
317   network based on U-Net (R2U-Net) for medical image segmentation[J]. arXiv preprint
318   arXiv:1802. 06955, 2018.
319   [6]LI X, CHEN H, QI X, et al. H-DenseUNet: hybrid densely connected UNet for liver and
320   tumor segmentation from CT volumes[J]. IEEE Transactions on Medical Imaging, 2018, 37(12):
321   2663-2674.
322   [7]IZADI S, MIRIKHARAJI Z, KAWAHARA J, et al. Generative adversarial networks to
323   segment skin lesions[C]//2018 IEEE 15th International Symposium on Biomedical Imaging
324   (ISBI 2018). IEEE, 2018: 881-884.
325   [8]XIE X, NIU J, LIU X, et al. A survey on incorporating domain knowledge into deep learning
326   for medical image analysis[J]. Medical Image Analysis, 2021: 101985.
327   [9]BERGER L, EOIN H, CARDOSO M J, et al. An adaptive sampling scheme to efficiently
328   train fully convolutional networks for semantic segmentation[C]//Annual Conference on Medical
329   Image Understanding and Analysis. Springer, Cham, 2018: 277-286.

330   [10]WU B, ZHOU Z, WANG J, et al. Joint learning for pulmonary nodule segmentation,
331   attributes and malignancy prediction[C]//2018 IEEE 15th International Symposium on
332   Biomedical Imaging (ISBI 2018). IEEE, 2018: 1109-1113.
333   [11]MIRIKHARIJI Z, HAMARNEH G. Star shape prior in fully convolutional networks for
334   skin lesion segmentation[C]//International Conference on Medical Image Computing and
335   Computer-Assisted Intervention. Springer, Cham, 2018: 737-745.
336   [12]ZHANG J, PETITJEAN C, AINOUZ S. Kappa loss for skin lesion segmentation in fully
337   convolutional network[C]//2020 IEEE 17th International Symposium on Biomedical Imaging
338   (ISBI). IEEE, 2020: 2001-2004.
339   [13]LIN T Y, GOYAL P, GIRSHICK R, et al. Focal loss for dense object
340   detection[C]//Proceedings of the IEEE international conference on computer vision. 2017: 2980-
341   2988.
342   [14]ZHU X, ZHOU H, YANG C, et al. Penalizing top performers: Conservative loss for
343   semantic segmentation adaptation[C]//Proceedings of the European Conference on Computer
344   Vision (ECCV). 2018: 568-583.
345   [15]EL JURDI R, PETITJEAN C, HONEINE P, et al. High-level prior-based loss functions for
346   medical image segmentation: A survey[J]. Computer Vision and Image Understanding, 2021,
347   210: 103248.
348   [16]PAINCHAUD N, SKANDARANI Y, JUDGE T, et al. Cardiac MRI segmentation with
349   strong anatomical guarantees[C]//International Conference on Medical Image Computing and
350   Computer-Assisted Intervention. Springer, Cham, 2019: 632-640.
351   [17]CHEN C, BIFFI C, TARRONI G, et al. Learning shape priors for robust cardiac MR
352   segmentation from multi-view images[C]//International Conference on Medical Image
353   Computing and Computer-Assisted Intervention. Springer, Cham, 2019: 523-531.
354   [18]ISIC Melanoma Data set[EB/OL]. [2020-05-28]. https://www. isic-archive.
355   com/#!/onlyHeaderTop/gallery.
356   [19]PASZKE A, GROSS S, MASSA F, et al. Pytorch: An imperative style, high-performance
357   deep learning library[J]. Advances in neural information processing systems, 2019, 32: 8026-
358   8037.
359   [20]RUSSAKOVSKY O, DENG J, SU H, et al. Imagenet large scale visual recognition
360   challenge[J]. International journal of computer vision, 2015, 115(3): 211-252.
361   [21]LOSHCHILOV I, HUTTER F. Decoupled weight decay regularization[J]. arXiv preprint
362   arXiv:1711. 05101, 2017.
363   [22]JÉGOU S, DROZDZAL M, VAZQUEZ D, et al. The one hundred layers tiramisu: Fully
364   convolutional densenets for semantic segmentation[C]//Proceedings of the IEEE Conference on
365   Computer Vision and Pattern Recognition Workshops. 2017: 11-19.
366   [23]GOCERI E. Deep learning based classification of facial dermatological disorders[J].
367   Computers in Biology and Medicine, 2021, 128: 104118.
368   [24]GOCERI E. Fully automated and adaptive intensity normalization using statistical features
369   for brain MR images[J]. Celal Bayar University Journal of Science, 2018, 14(1): 125-134.

Figure 1

Figure 1 The internal hole error and external island error in partition diagram
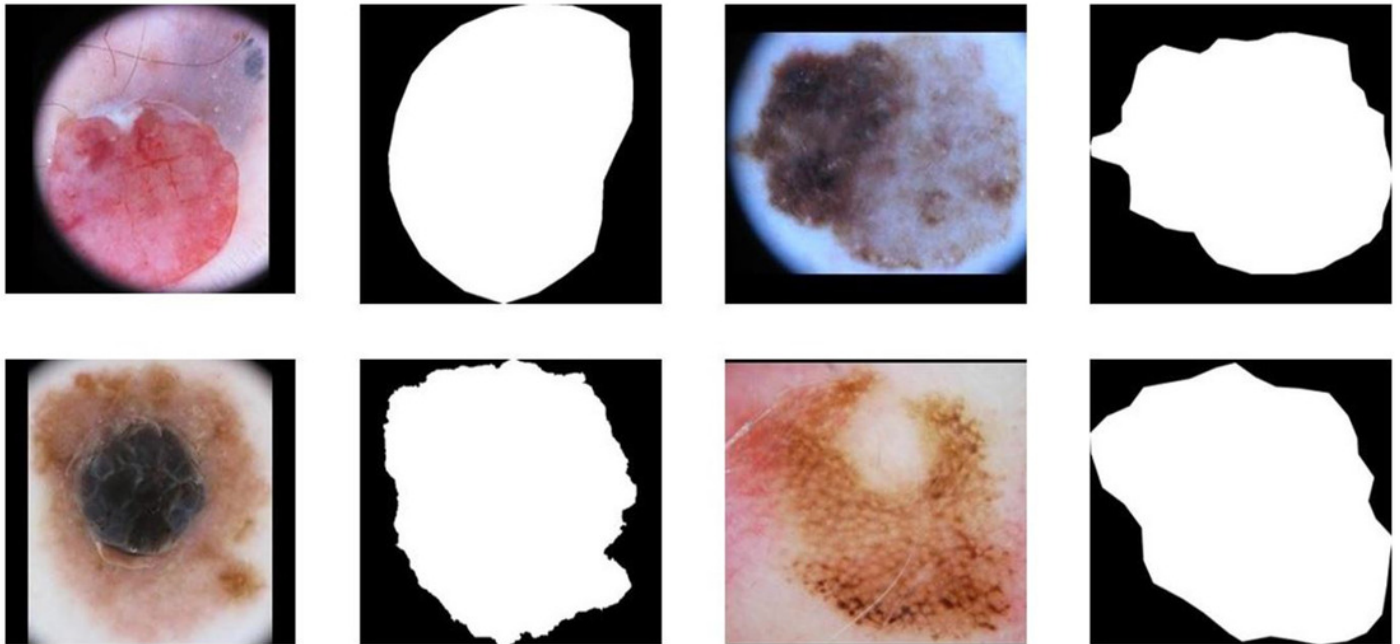
Figure 2

Figure 2 The original image and segmentation label of melanoma image
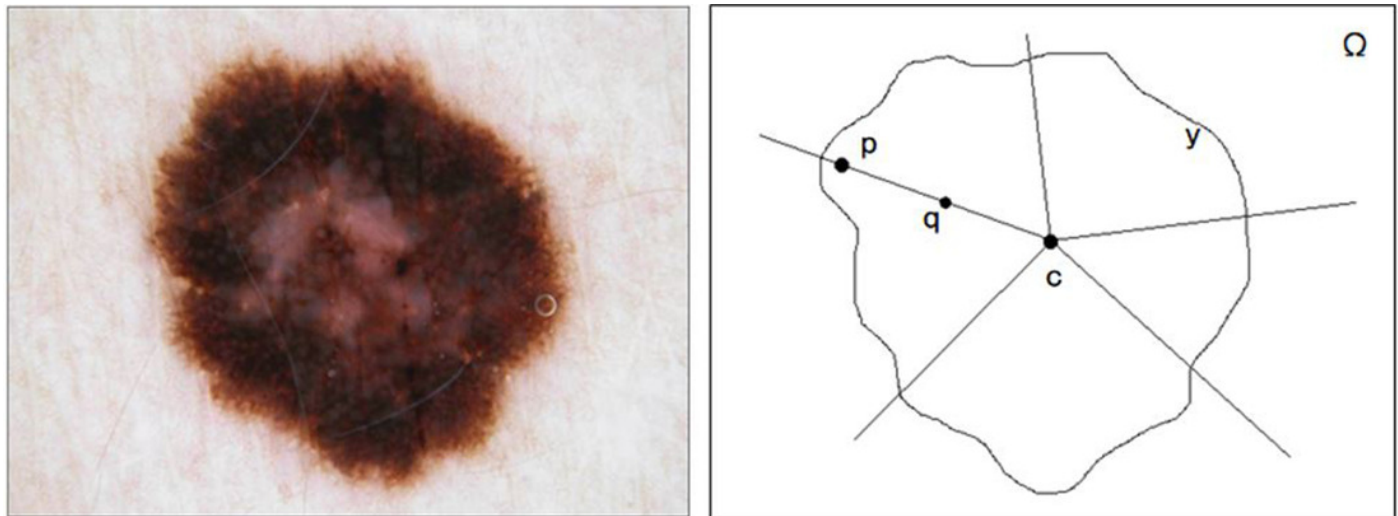
Figure 3

Figure 3 Schematic of a star convex set in a melanoma image sample
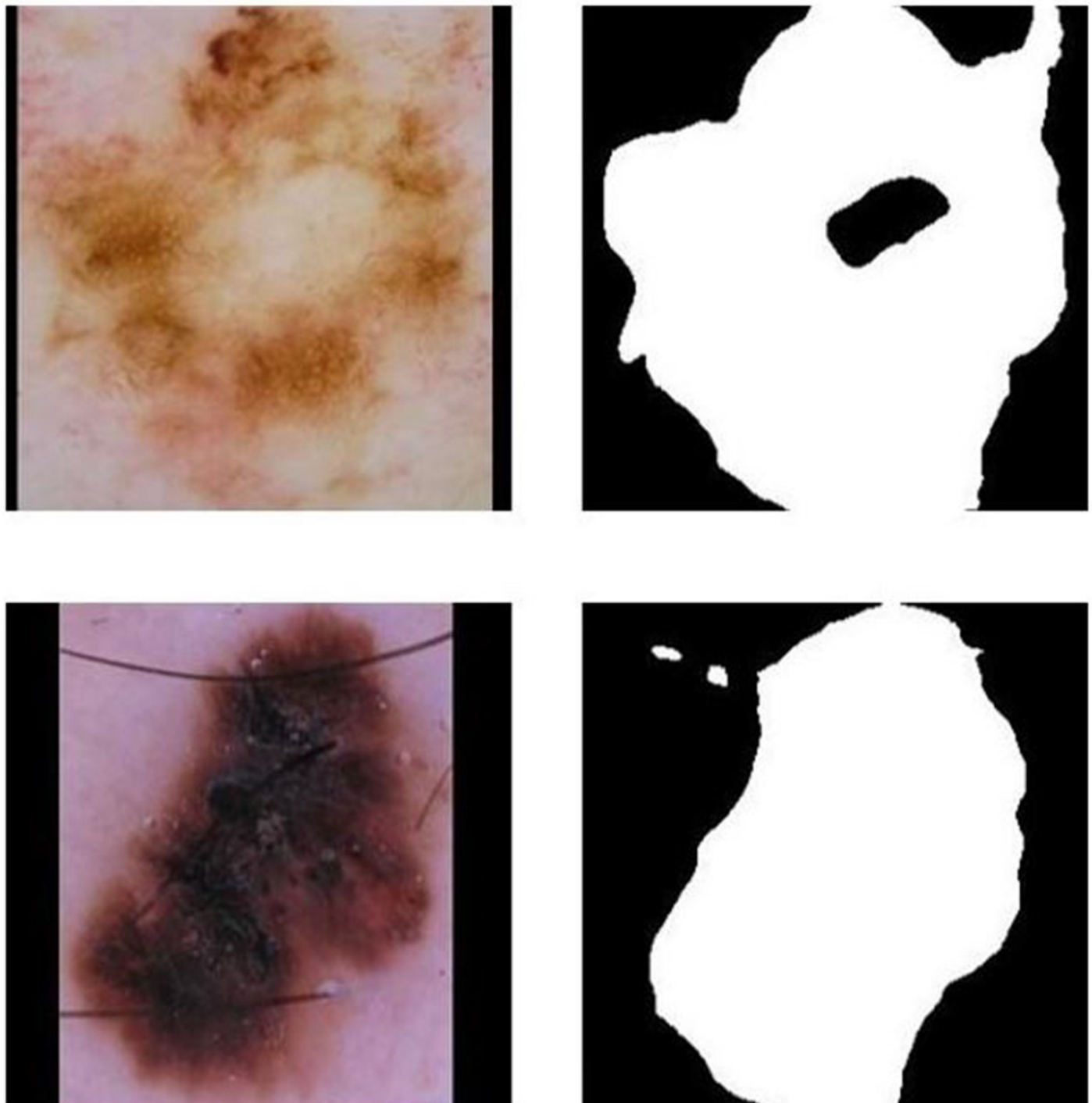
Figure 4

Figure 4 UNet network model based on ResNet34 network structure
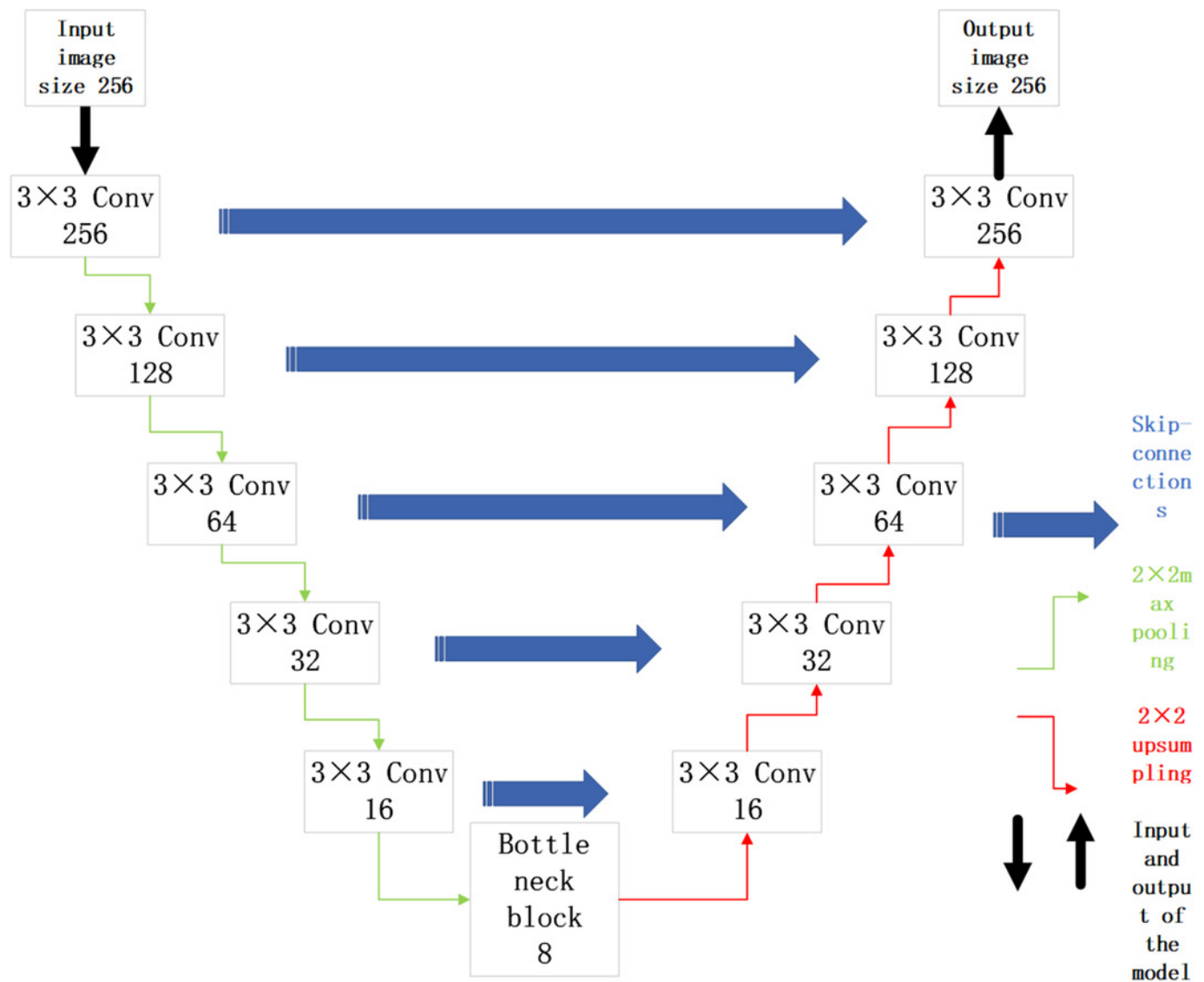
Figure 5

Figure 5 Determine whether point q is an internal hole

(a)Segmentation label of melanoma image (b)Schematic diagram of model prediction
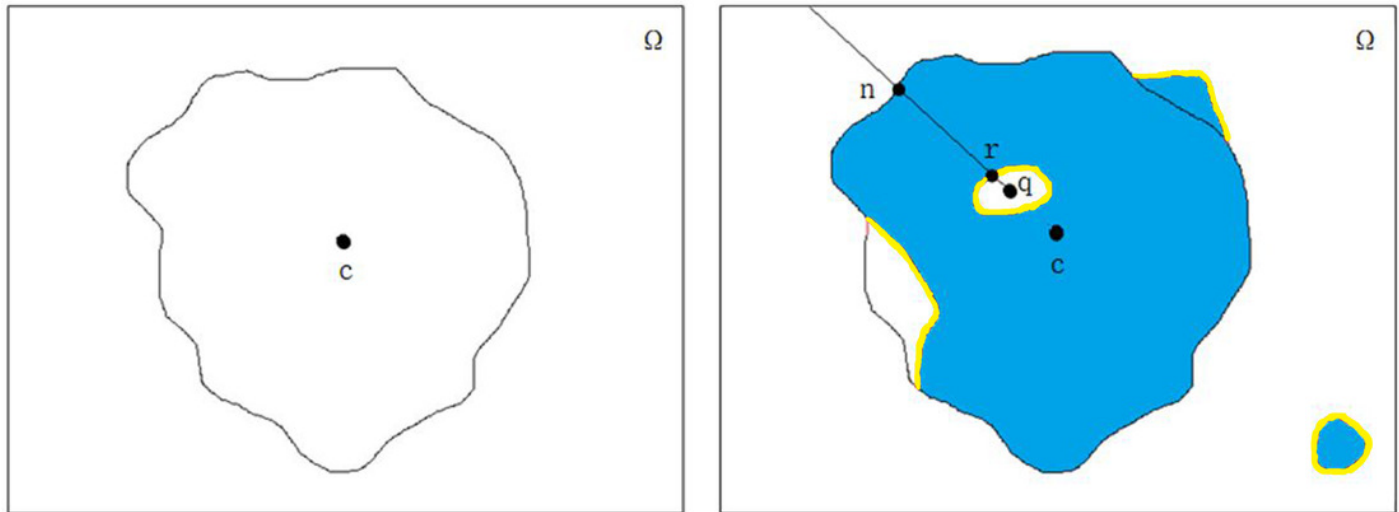
Figure 6

Figure 6 Diûerent types of segmentation errors
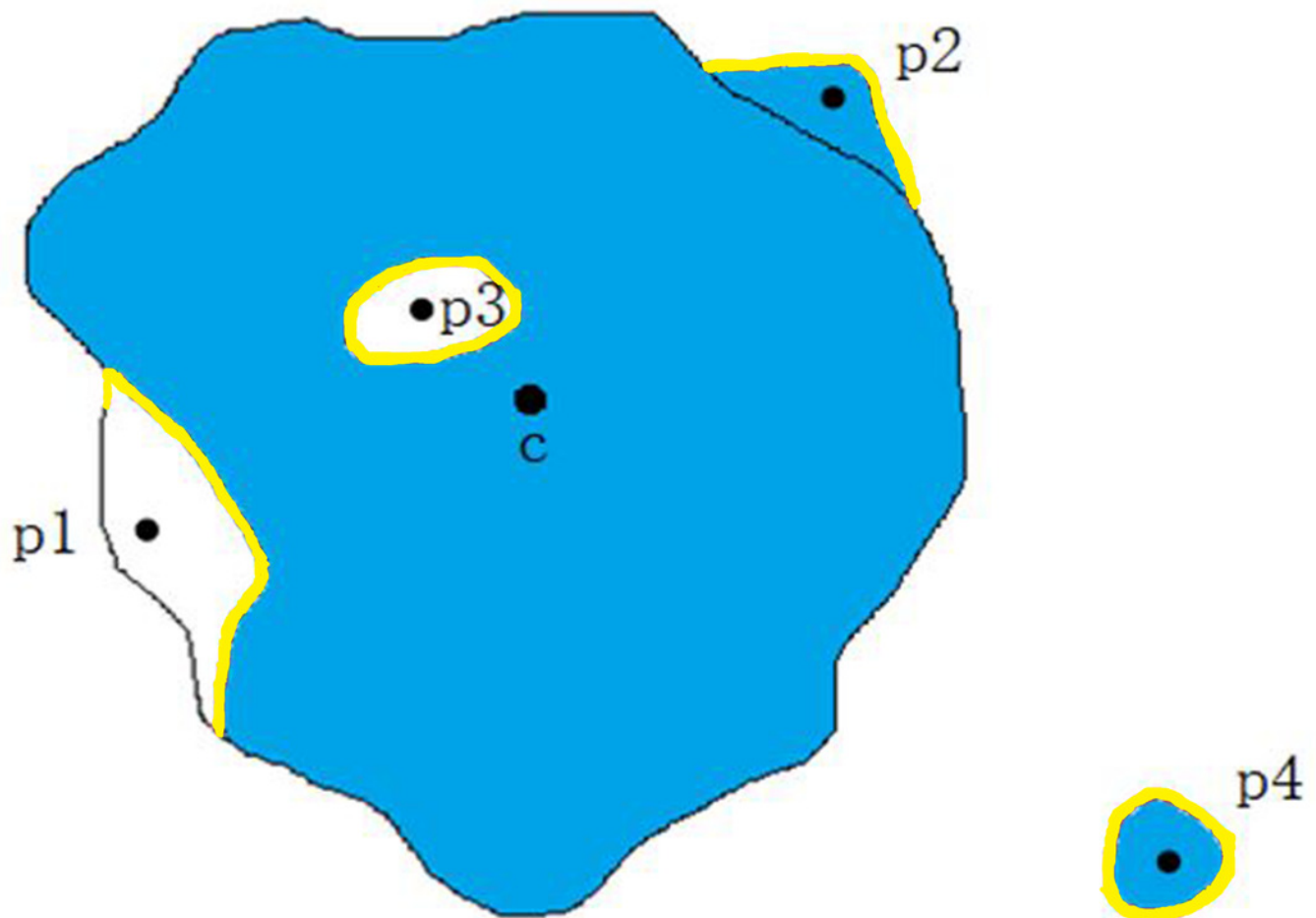
Figure 7

Figure 7 Malignant samples after preprocessing

(a) Sample 0155 after preprocessing

(b) Sample 0144 after preprocessing

(c) Sample 0169 after preprocessing
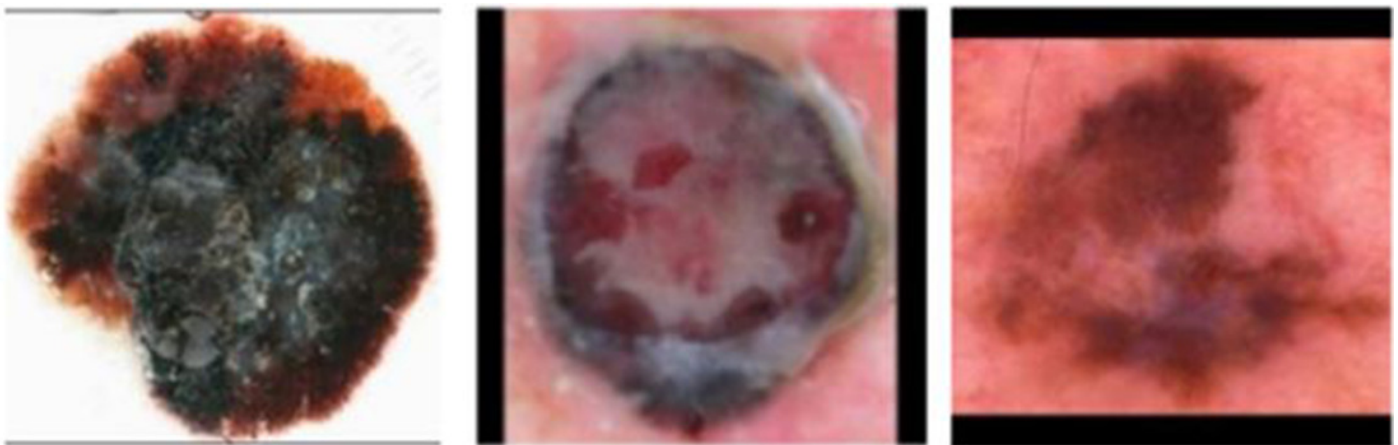
Figure 8

Figure 8 Ablation experiment segmentation results display

(a) The original image 1138 (b) Segmentation label (c) Non-regular item group (d) Unsegmented star prior group (e) Non-center distance scaling group (f) Segmented star prior group
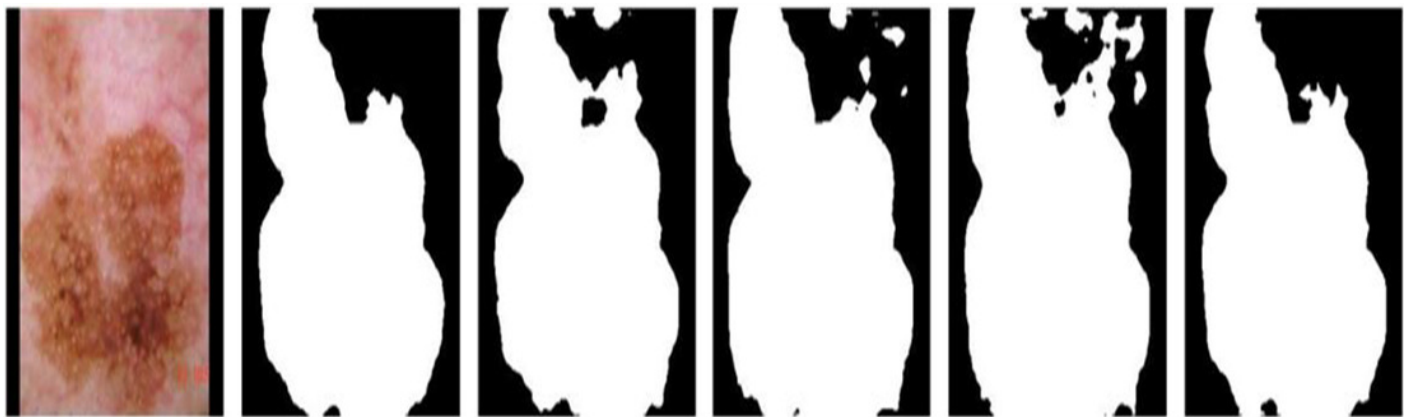
Tab 1 The experimental results

Tab 1 The experimental results

The experimental group	Choice of L_{ce} function	Parameter Settings				mIoU (%)	mAP (%)	Dice (%)	Jaccard (%)
		Item L_{ce} weight α	Item L_{sh} weight β	item A weight μ	item B weight ρ				
Non-regular item (baseline) group	Cross entropy loss	None	None	None	None	85.10	92.56	92.68	86.76
	Dice loss	None	None	None	None	85.72	92.61	92.89	86.95
Unsegmented star prior group	Cross entropy loss	1	0.01	None	None	85.31	92.61	92.86	86.98
	Dice loss	1	0.01	None	None	85.90	92.65	93.10	87.18
non-Center distance scaling group	Cross entropy loss	1	0.33	0.02	0.05	84.97	92.57	92.79	86.78
				0.02	0.1	84.79	92.50	92.71	86.65
	Dice loss	1	0.33	0.02	0.05	85.42	92.61	92.97	87.01
				0.02	0.1	85.38	92.56	92.92	86.85
Segmented star prior group	Cross entropy loss	1	0.33	0.1	0.5	86.48	92.89	93.05	87.22
				0.1	1	86.78	93.08	93.22	87.50
	Dice loss	**1**	**0.33**	0.1	0.5	87.09	92.95	93.26	87.40
				0.1	**1**	**87.41**	**93.13**	**93.49**	**87.69**

Tab 2 Results of different methods

Tab 2 Results of different methods

model	mIoU(%)	mAP(%)	Dice(%)	Jaccard(%)
UNet	86.00	92.53	92.97	87.09
FC-DenseNet	85.92	92.66	93.04	87.12
SSPFCN	85.90	92.65	93.10	87.18
Attention UNet	86.56	92.76	93.16	87.35
Our method	**87.41**	**93.13**	**93.49**	**87.69**